Supporting Information:

The nanocrystal superlattice anvil cell: a method to study molecular bundles under uniaxial compression

Kaifu Bian,[a] Arunima Singh,[b] Richard G. Hennig,[b] Zhongwu Wang,[c] and Tobias Hanrath,[a,*]

[a]School of Chemical and Biomolecular Engineering, [b]Department of Material Sciences and Engineering, [c]Cornell High Energy Synchrotron Source (CHESS), Cornell University, Ithaca, NY, 14853 [*]Corresponding Author

1. Experimental Methods

Synthesis of Colloidal PbS Nanocrystals

PbS nanocrystals used in this study were prepared using the method reported by Hines and Scholes [1]. In a typical synthesis, 0.45 g of lead oxide was dissolved in 20 mL of oleic acid (OA) to form lead oleate solution. Then the solution was heated to 150 ℃ for one hour under nitrogen flow to form a lead oleate solution. The solution was then cooled down to 130 ℃. In a nitrogen glovebox, 210 μL of bis(trimethylsilyl)sulfide (TMS) was dissolved in 10 mL of 1-octadecene (ODE) and stirred thoroughly and then injected rapidly into the vigorously stirred, hot lead oleate solution. The mixture turned dark immediately after injection indicating the formation of PbS NCs. NCs were collected after reaction for 1 min then washed twice by sequential precipitation with ethanol and redispersion in hexane. Finally the solvent was removed by nitrogen flow and dry NCs were stored inside the nitrogen glovebox (oxygen <1 ppm).

NC Size Measurements by Transmission Electron Microscopy.

PbS NCs were dispersed in hexane and drop-cast on carbon coated copper grids for transmission electron microscopy (TEM) imaging using a FEI Tecnai T-12 microscope operated at 120 kV. The average diameter of NCs is determined by statistics on 300 NCs in multiple TEM images. Figure S1 show a representative TEM image and the corresponding diameter histogram of the PbS NCs. The size of the PbS NCs is determined to be $d_0 = 6.3 \pm 0.5$ nm in diameter.

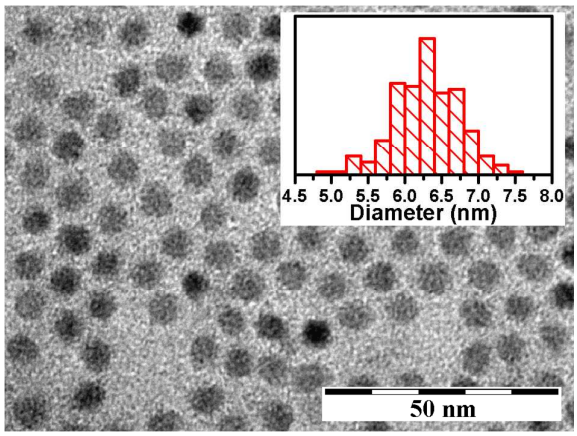

Figure S1. TEM image of the PbS NCs. Insets shows histogram of NC diameter by counting 300 NCs.

NC Superlattice Formation and Ligand Exchange

PbS NC thin films were prepared under room conditions by drop casting PbS NC suspension (~ 20 mg/mL) on diced and cleaned silicon wafers of ~10x10 mm. For each sample, approximately 5 mg of NC was deposited.

The samples studied in high-pressure measurements were prepared by soaking NC thin films in 0.1 M acetonitrile (ACN) solutions of ethanedithiol (EDT), butanedithiol (BDT) or hexanedithiol (HDT) for ligand exchange. During the process, the original oleic acid ligands on PbS NC surface were replace by alkanedithiol linkers that form bundles connecting neighboring NCs. To ensure complete ligand exchange, the samples were exposed to the ligand exchange solution for four days and afterward rinsed by ACN twice and then soaked in ACN for one extra day to remove possible residual non-chemisorbed ligands followed by drying in air. These three samples are denoted as EDT, BDT and HDT. One NC film with native oleic acid ligands was left untreated as a control sample and denoted as OA.

in-situ High-Pressure X-ray Scattering measurements.

High pressure was achieved by a diamond anvil cell (DAC) consisting of two aligned diamond anvils. A small piece of alkanedithiol-exchanged PbS NC film was loaded into a 150-μm diameter hole drilled on a pre-indented stainless-steel gasket and then encapsulated and pressurized by the diamond anvils (Figure 1a). Multiple ruby chips were placed in the gasket in the DAC with the sample to measure pressure using a well-known standard pressure dependent ruby fluorescence method. The high-pressure experiments were done in absence of a pressure transmitting medium. The pressure gradient within the sample chamber never exceeded 0.2 GPa in all measurements in this work.

High-pressure X-ray scattering measurements were performed at the B1 beamline at Cornell High Energy Synchrotron Source (CHESS). A monochromatic X-ray of wavelength of 0.4859 Å was generated by two Ge (111) single crystals. Then the beam size was reduced to 100 μm by a collimator. Both SAXS and WAXS patterns from the samples were simultaneously collected by a large-area Mar345 image plate

detector. The sample-to-detector distance was calibrated using a CeO_2 standard to 784.8 mm. The scattering patterns were then integrated by Fit2D software[2] and analyzed.

2. Calculation of interparticle separation, δ_{nn} and comparison with free linker chain length l_0

We fitted the first and strongest peak in the SAXS pattern (Figure 2) taken at ambient pressure to a Lorentzian peak to determine the center of the peak q_{SAXS}. The average e separation between nearest neighboring NC surfaces, δ_{nn} in the superlattice can be calculated by subtracting the NC diameter from the center-to-center spacing [3]:

$$\delta_{nn}=\frac{\sqrt{3}}{\sqrt{2}}\frac{2\pi}{q_{SAXS}}-d_0 \qquad \text{(S1)}$$

Where d_0 = 63Å is the mean diameter of the PbS NC cores. The calculated δ_{nn} in each sample are listed in Table S1 and plotted in Figure S2 to compare with the theoretical length of a free alkanedithiol linker molecule l_0 as defined by Figure 1d and calculated by the software Avogadro with universal force field.[4] This comparison indicates that upon ligand exchange, δ_{nn} is in reasonably good agreement with l_0 and confirms successful ligand exchanges in the three samples

Table S1. Calculated nearest neighboring NCs separation (δ_{NN}) comparing with length of free linker molecule chain (l_0)

Sample	δ_{nn} (Å)	l_0 (Å)
EDT	6.1	6.1
BDT	8.4	8.6
HDT	11.0	11.2

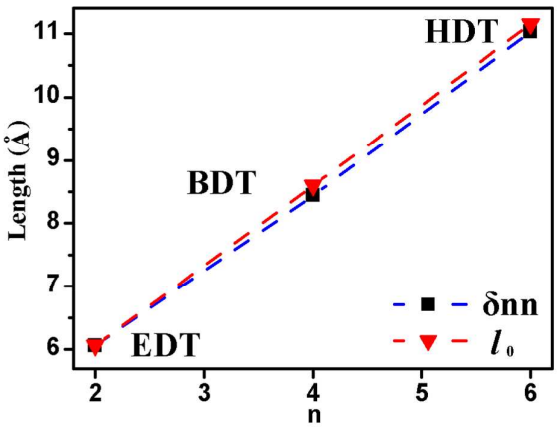

Figure S2. Comparing measured nearest neighboring NCs separation δ_{nn} with theoretical free alkanedithiol linker molecule chain length l_0.

3. *In-situ* high-pressure SAXS measurements

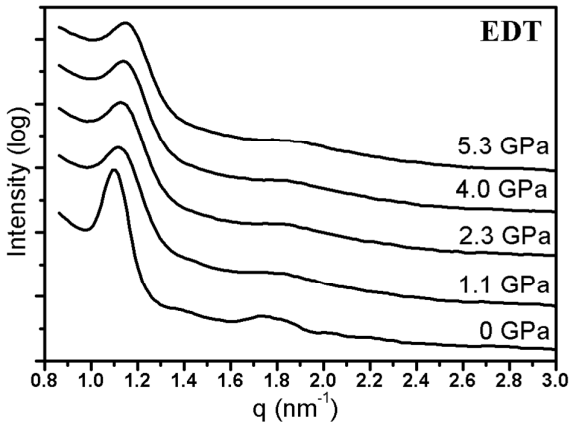

Figure S3. SAXS patterns of the EDT sample under elevated pressures

Figure S3 shows *in-situ* high-pressure SAXS data of the EDT sample as a representative. The shift of the SAXS peaks indicates the shrinkage of the NCSL. The center position of the first order, also the strongest, peak q_{SAXS} was found by fitting to a Lorentzian distribution after subtraction of background. The normalized unit cell volume of the NCSL $v_{SL}(p)$ was then calculated by eqn. S2 and fitted to Vinet equation of state (eqn. 1) to obtain the bulk moduli of the NCSLs (Figure 3a).

$$v_{SL}(p) = \frac{V_{SL}(p)}{V_{SL}(p=0)} = \left[\frac{q_{SAXS}(p=0)}{q_{SAXS}(p)}\right]^3 \quad \text{(S2)}$$

Where $V_{SL}(p)$ is the volume of a NCSL unit cell.

4. *In-situ* high-pressure WAXS measurements

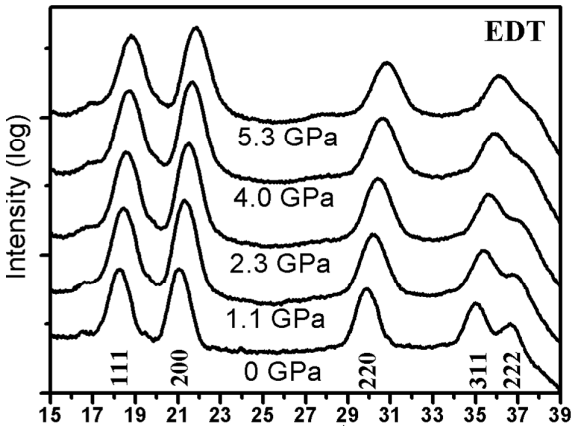

Figure S4. WAXS spectra of the EDT sample under elevated pressures. The peaks are labeled by their Miller indices

Figure S4 shows *in-situ* high-pressure WAXS data of the EDT sample as an example. The shift of the WAXS peaks indicates the compression of PbS NC cores. To calculate bulk moduli of the PbS NC cores, the first four WAXS peaks ({111}, {200}, {220}

and {311} of rock salt lattice) in each WAXS spectrum were determined. The peak positions were used to obtain the lattice parameter $a_{NC}(p)$ by the software UnitCell based on a minimum square error method.[5] Then the normalized unit cell volume of the PbS atomic lattice $v_{NC}(p)$, which is equivalent to the normalized total volume of a NC core, was calculated from $a_{NC}(p)$ by eqn. S3 and fitted to Vinet equation of state (eqn. 1) to obtain the bulk moduli of the NCSLs (Figure 3b).

$$v_{NC}(p) = \frac{V_{NC}(p)}{V_{NC}(p=0)} = \left[\frac{a_{NC}(p)}{a_{NC}(p=0)}\right]^3 \quad \text{(S3)}$$

Where $V_{NC}(p)$ is the volume of a unit cell of PbS atomic lattice in the NC cores.

5. Comparing Initial PbS Lattice Expansions

Table S2. Comparing PbS atomic lattice expansions in alkanedithiol-treated samples with control sample and bulk values

Sample	d_{111} (Å)	d_{200} (Å)	a_{NC} (Å)	Expansion (‰)
Bulk	3.420	2.962	5.924	0
OA	3.434	2.980	5.936	2.0
EDT	3.443	2.982	5.951	4.6
BDT	3.428	2.987	5.942	3.0
HDT	3.423	2.989	5.945	3.5

Table S2 compares the atomic {111} and {200} spacings and lattice parameter a_{NC} of the three alkanedithiol treated samples (OA) with those of an untreated sample as well as bulk values. The expansion rates with respect to bulk are also provided. The results shows that comparing with bulk values, the PbS atomic lattice displays clear lattice expansion which agrees with our previous work.[6] The expansion rate in different NC samples varies due to different surface chemistry. And the initial lattice expansion in the EDT sample is considerably larger than in the others. This extra lattice expansion might cause the difference in bulk moduli of the three samples (Table1 and Figure 2b). Investigations on the lattice expansion and its relationship to the hardness of NCs are still in progress and will be reported in a future paper.

6. Calculation of the elastic module *K* by DFT Simulations

To determine the elastic module *K* of the alkanedithiol linker molecules involved in this study, DFT simulations have been performed on compression of individual alkanedithiol molecules. The alkanedithiol (xDT) molecules were modeled as Pb-xDT-Pb molecules in a periodic cell of 25Å x 25 Å x 25 Å containing the xDT molecules with 10, 16 and 22 atoms, respectively, as shown in Figure S5. Compression was modeled by reducing the distance between the terminal lead atoms, followed by relaxation of the atomic positions of the remaining atoms. Force exerted by the compressed molecule is the product of pressure on the plane perpendicular to the molecular axis and the area of that plane. The "spring constant" for each xDT molecules is calculated from the slope of force-length curves, where length is length of the Pb-xDT-Pb chain. Figure S6 shows the DFT results which were then used to predict the elastic module $K = -\lim_{\Delta l \to 0} f/\varepsilon$ by taking the slope of the force-strain curve at $F = 0$. The calculated values of *K* are listed in Table 1.

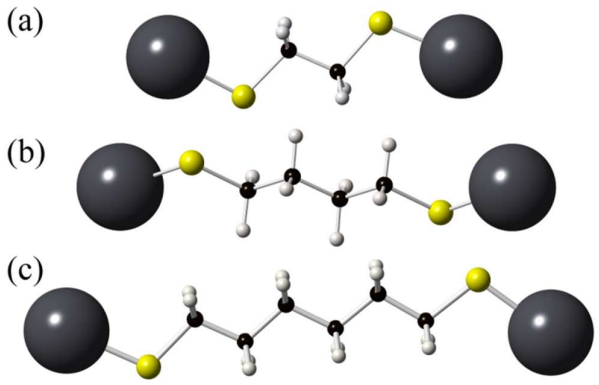

Figure S5. DFT structure of Pb-xDT-Pb chains used for computing the elastic module *K* for a) EDT, b) BDT and c) HDT.

The DFT calculations were performed using the Vienna Ab-initio Simulation Package (VASP)[7-9] using the projector augmented wave (PAW) method[10,11] and the Perdew-Burke-Ernzerhof (PBE)[12,13] exchange correlation functional. The cut-off energy for the plane-wave basis set was set to 400 eV. The relaxations of the atoms were carried out with the conjugate-gradient algorithm scheme, until the maximum force on any atom was below 0.05 eV/Å. The Brillouin zone integrals were performed using a uniform *k*-point mesh with a density of at least 20 per $Å^{-1}$ and a Gaussian smearing of 0.2 eV.

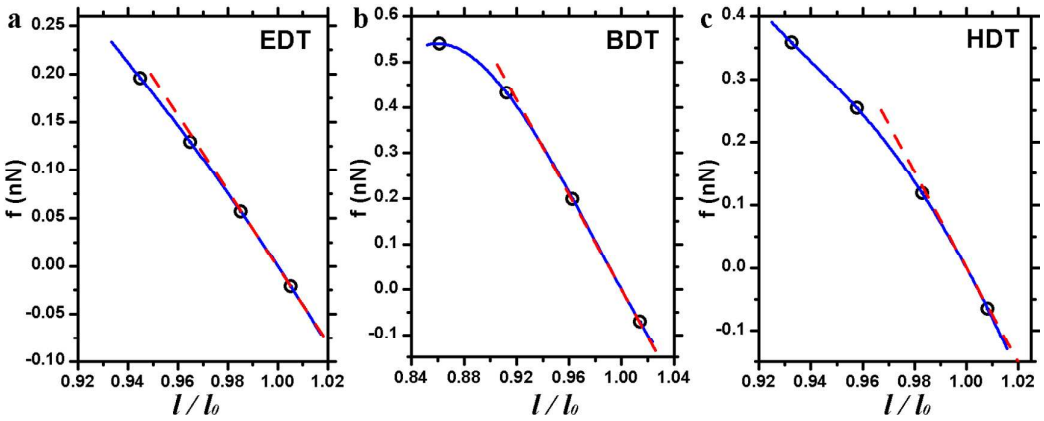

Figure S6. Results of DFT simulations on compression of single molecule chain of (a) EDT, (b) BDT and (c) HDT. The blue curves are spline fits of the data. The red dashed lines indicates the slope at $f = 0$.

7. Modeling the Compression of NCSL

To correlate the measured bulk moduli B_0 of both NCSL and PbS cores to the hardness of the linker molecules by DFT simulations, we modeled the system under an infinitesimally small pressure ($p \rightarrow 0^+$) starting from the center-to-center distance between nearest-neighbor NCs in a SL d_{nn}.

$$d_{nn}(p) = d(p) + l(p) \tag{S4}$$

The pressure p can be related to f and σ by

$$p = \frac{F}{A} = \frac{F}{m/\sigma} = f\sigma \tag{S5}$$

Where F is the total force applied on a linker bundle connecting the neighboring NCs (Figure 1c), A is the surface area on a NC taken by each bundle, m is the number of alkanedithiol molecules in a bundle, σ is NC surface linker density. By taking derivative of eqn. S4, we have

$$\left.\frac{dd_{nn}}{dp}\right|_{p=0} = \left.\frac{dd}{dp}\right|_{p=0} + \left.\frac{dl}{dp}\right|_{p=0} \tag{S6}$$

The superlattice term on the LHS of eqn. S6 can be related to the bulk modulus of the NCSL $B_{0,SL}$ by

$$\frac{1}{B_{0,SL}} = -\left.\frac{dv_{SL}}{dp}\right|_{p=0} = -d\left(\frac{d_{nn}}{d_{nn,0}}\right)^3 \Big/ \left.dp\right|_{p=0} = -\frac{3}{d_{nn,0}}\left.\frac{dd_{nn}}{dp}\right|_{p=0} \tag{S7}$$

Then it becomes

$$\left.\frac{dd_{nn}}{dp}\right|_{p=0} = -\frac{d_{nn,0}}{3B_{0,SL}} = -\frac{l_0 + d_0}{3B_{0,SL}} \tag{S8}$$

Similarly, the NC core term in eqn. S6 can be rewritten as

$$\left.\frac{dd}{dp}\right|_{p=0} = -\frac{d_0}{3B_{0,NC}} \tag{S9}$$

For the linker term, using eqn. S5 we have

$$\left.\frac{dl}{dp}\right|_{p=0} = \left.\frac{l_0 d\varepsilon}{\sigma df}\right|_{p=0} = \frac{l_0}{\sigma}\lim_{\Delta l \to 0}\frac{\Delta\varepsilon}{f} = -\frac{l_0}{\sigma K} \tag{S10}$$

Now we have the following overall expression of the NCSL compression by plugging eqn. S8-10 into S6.

$$\frac{d_0 + l_0}{B_{0,SL}} = \frac{d_0}{B_{0,NC}} + \frac{3l_0}{K\sigma} \tag{S11}$$

Eqn. S11 clearly show that the compression of both NC cores and interstitial linkers contribute to the shrinkage of the NCSL. And it was then used to calculate the surface linker density σ that listed in Table 1 in the main text.

8. Deriving the *f-l* relationship for molecular linkers in a bundle.

To obtain the force-length, *i.e. f(l)* relationship of molecular linkers in a bundle from experimental data we first convert measured pressure p into the force f using eqn. S5. Then l is calculated by

$$l(p) = d_{nn,0}\sqrt[3]{v_{SL}(p)} - d_0\sqrt[3]{v_{NC}(p)} \quad \text{(S12)}$$

v_{SL} and v_{NC} are adopted from SAXS and WAXS data respectively. Both measured data points and the corresponding Vinet EOS fits were processed in this way. And the results are shown in Figure 3 of the main text.

9. DFT Simulations of Compression of Alkanedithiol Linker Bundles in NCSL

The experimental compression of the linker bundles was mimicked in the simulation by attaching xDT molecules between two reconstructed PbS (111) surfaces (see Figure S7). The xDT linker bundles in NCSL were modeled as periodic models of single xDT ligand molecules attached along their axis perpendicular to 2x2 PbS (111) surface, yielding a ligand density of 1.6 nm^{-2}. A slab model was used to model the PbS (111) surface with four Pb-S layers. The lattice constant of bulk PbS was calculated to be 5.934 Å. The PbS (111) surface was reconstructed by moving half the Pb ions of the Pb-terminated (111) surface layer of the slab to the opposing S terminated surface [14]. The bulk geometry was used to fix the position of the Pb and S ions except for those on the top two layers to reduce elastic interaction between the periodic images. The atomic positions of all other atoms were relaxed keeping the simulation cell fixed.

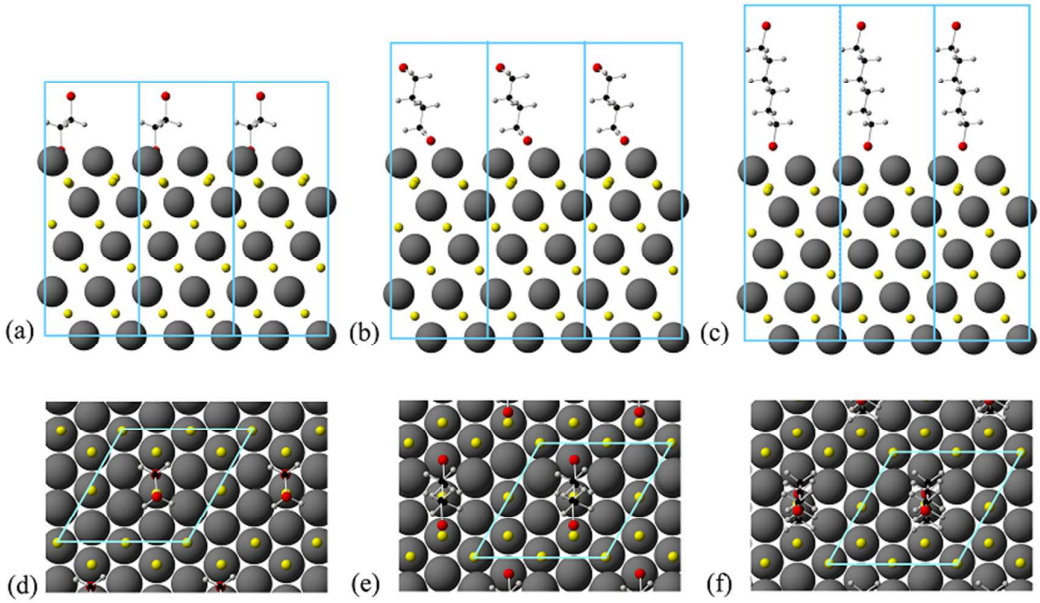

Figure S7. Side view, (a), (b) and (c) and top view, (d), (e) and (f) of simulation setup of linker molecules attached to reconstructed PbS (111) surfaces for EDT, BDT and HDT, respectively. The blue enclosures represent one unit cell. The red spheres for the terminal S atoms in the xDT molecules are used to distinguish from the yellow S atoms of the PbS (111) slab.

A fully relaxed geometry was compressed by reducing the height of the simulation box perpendicular to the PbS (111) surface, followed by relaxation of the atoms within this compressed simulation cell. The elastic force exerted by the xDT molecules is the product of the PbS (111) surface area and the component fo the stress tensor in the direction perpendicular to the PbS (111) surface. The length of xDT is approximated as the vertical distance between the two Pb atoms bonding to the S atoms of the xDT molecules. The results from the DFT simulation are shown in Figure 4 in main text.

References

(1) Hines, M. A.; Scholes, G. D. *Adv. Mater.* **2003**, *15*, 1844.

(2) Hammersley, A. P. *ESRF Internal Report, ESRF97HA02T* **1997**.

(3) Wang, Z.; Schliehe, C.; Bian, K.; Dale, D.; Bassett, W. A.; Hanrath, T.; Klinke, C.; Weller, H. *Nano Letters* **2013**, *13*, 1303.

(4) Hanwell, M. D.; Curtis, D. E.; Lonie, D. C.; Vandermeersch, T.; Zurek, E.; Hutchison, G. R. *Journal of Cheminformatics* **2012**, ***4***.

(5) Holland, T. J. B.; Redfern, S. A. T. *Mineralogical Magazine* **1997**, *61*, 65.

(6) Bian, K.; Wang, Z.; Hanrath, T. *J. Am. Chem. Soc.* **2012**, *134*, 10787.

(7) Kresse, G.; Hafner, J. *Phys. Rev. B* **1993**, *47*, 558.

(8) Kresse, G.; Hafner, J. *Phys. Rev. B* **1994**, *49*, 14251.

(9) Kresse, G.; Furthmüller, J. *Comput. Mat. Sci* **1996**, *6*, 15.

(10) Blochl, P. E. *Phys. Rev. B* **1994**, *50*, 17953.

(11) Kresse, G.; Joubert, D. *Phys. Rev. B* **1999**, *59*, 1758.

(12) Perdew, J. P.; Burke, K.; Ernzerhof, M. *Phys. Rev. Lett.* **1996**, *77*, 3865.

(13) Perdew, J. P.; Burke, K.; Ernzerhof, M. *Phys. Rev. Lett.* **1997**, *78*, 1396.

(14) Bealing, C. R.; Baumgardner, W. J.; Choi, J. J.; Hanrath, T.; Hennig, R. G. *ACS Nano* **2012**, *6*, 2118.